# Preparation and Characterization of Konjac Glucomannan/Poly(diallydimethylammonium chloride) Blend Films

**Jun Lu,[1,3] Jinhua Zhang,[2] Chaobo Xiao[1]**

[1]*College of Chemistry and Molecular Sciences, Wuhan University, Wuhan 430072, People's Republic of China*
[2]*College of Chemistry, Huazhong Agricultural University, Wuhan 430070, People's Republic of China*
[3]*College of Chemistry and Bioscience, Xiangfan University, Xiangfan 441003, People's Republic of China*

Received 26 December 2006; accepted 10 May 2007
DOI 10.1002/app.26732
Published online 20 July 2007 in Wiley InterScience (www.interscience.wiley.com).

**ABSTRACT:** A novel preservative film was prepared by blending konjac glucomannan (KGM) and poly (diallydimethylammonium chloride) (PDADMAC) in aqueous system. The effects of PDADMAC content on the miscibility, morphology, thermal stability, and mechanical properties of the blend films were investigated by density determination, scanning electron microscopy (SEM), attenuated total reflection infrared spectroscopy (ATR-IR), X-ray diffraction (XRD), differential scanning calorimetry (DSC), thermogravimetric analysis (TGA), and tensile tests. The results of the density determination predicted that the blends of KGM and PDADMAC were miscible when the PDADMAC content was less than 70 wt %. Moreover, SEM and XRD confirmed the result. ATR-IR showed that strong intermolecular hydrogen bonds interaction occurred between the negative charge groups of KGM and the quaternary ammonium groups of PDADMAC in the blends. The tensile strength and the break elongation of the blends were improved largely to 106.5 MPa and 32.04%, when the PDADMAC content was 20 wt %. The thermal stability of the blends was higher than pure KGM. Results from the film-coating preservation experiments with lichi and grapes showed that the blend film had excellent water-holding and preservative ability. © 2007 Wiley Periodicals, Inc. J Appl Polym Sci 106: 1972–1981, 2007

**Key words:** KGM; PDADMAC; blending; cationic polyelectrolyte; structure; performance

## INTRODUCTION

There is an ever-increasing interest in the utilization of renewable and biodegradable materials. Among natural polymers, Konjac glucomannan (KGM) has attracted great interests, since it exhibits expected properties, such as easily modification and excellent film-forming ability, besides availability, low cost, good biocompatibility, and biodegradability. KGM, one of the a high molecular weight water-soluble nonionic natural polysaccharide found in tubers of the *Amorphophallus konjac*, is composed of β-(1→4)linked D-glucose and D-mannose in the molar ratio of 1 : 1.6 with a low degree of acetyl groups.[1] It has wide applications in food[2–4] and biomedical[5–9] domains. Although a good film-forming material candidate for food and fruit preservation, KGM has the common flaw of natural polymers, low mechanical properties and poor antimicrobial activity. Therefore, extensive research on the subject has been carried out.[10–12] Low molecular weight antibacterial substances were intermingled into materials, but the active substances could be diffused inadequately into the bulk of food.[13,14] Furthermore, chemically modified KGM cannot avoid the negative effect on mechanical properties.[15] In our early work,[16] we found that blending is a convenient and effective method of improving the performance of films. There were many reports about the blend film of KGM and other natural polymers,[17–19] but little about KGM and synthetic polymers with functional groups.[20] In the use of the functional blend, a safety problem must be solved because of the remained toxic monomer in synthetic polymers. Inspired from those studies, we selected poly(diallydimethylammonium chloride) (PDADMAC) as the partner with KGM and investigated the properties of KGM/PDADMAC films.

PDADMAC, the first synthetic polymer to be approved by the U.S. Food and Drug Administration for the use in potable water treatment, possesses a backbone of cyclic units and highly hydrophilic permanently charged quaternary ammonium groups. It is safe to human's health and has wide uses in paper manufacturing, water treatment industry, mining industry, and biological, medical, and food

*Correspondence to:* C. Xiao (cbxiaowhu@126.com).
Contract grant sponsor: Education Office of Hubei Province, People's Republic of China; contract grant numbers: D200525003, D200625004.

processes.[21] It belongs to strong cationic polyelectrolytes and has high water solubility, but there is little research on its antibacterial activity though it has quaternary ammonium groups.

Since good miscibility and performance is needed to blend materials, this work was focused on the effects of PDADMAC content on the miscibility and performance of the blend films. Density determination, SEM, ATR-IR, XRD, DSC, TGA, tensile tests, and preservation experiments were carried out. We predict that this work may contribute basic information to the further application of KGM and PDADMAC in packaging films and biomedical materials.

## EXPERIMENTAL

### Materials

KGM powder (purity 99%) was purchased from Huaxianzi Konjac (Hubei, China) and was used without further purification. The viscosity is 10 Pa s in 1 wt % concentration. DADMAC (65 wt % solution in water) monomer were supplied by Wuhan Jiangrun Fine Chemical; Ammonium peroxydisulfate (APS), sodium thiosulfate pentahydrate (STP), and ethylenediamine-tetraacetic acid disodium salt (EDTA) were purchased from Shantou Xilong Chemical Factory (Guangdong, China). All other chemicals were reagent grade and used without further purification.

### Synthesis of PDADMAC

PDADMAC was prepared by radical polymerization according to the following method: the DADMAC monomers were polymerized at 60°C for 5 h under a $N_2$ atmosphere, by using APS/STP and EDTA as initiator and accelerator, respectively. The contents of the initiator were that APS were 0.2 wt % of monomers and sodium thiosulfate were 0.15 wt % of monomers. The contents of the accelerator were 0.08 wt % of monomers. The resulting viscous solution was poured into an open beaker containing proper methanol/acetone (v/v 1:5). The white solid polymer was deposited and poured into the glass plate, then dried under vacuum at 40°C until constant weight, and stored in desiccators. Figure 1 shows the cyclopolymerization of the DADMAC monomer and the structure of the PDADMAC. The intrinsic viscosity ([η]) of the PDADMAC was determined by an Ubbelohde capillary viscometer (Chinese Academy of Sciences, China) at (25 ± 0.1)°C, using 0.5*M* NaCl as solvent. The value of [η] was 123.7 mL $g^{-1}$, calculated from Figure 2, which was the intercept of the curve of $\eta_{sp}/C$ versus *C*.

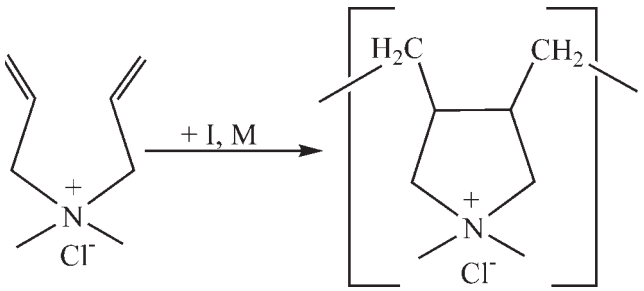


**Figure 1** Cyclopolymerization of DADMAC and the structure of PDADMAC.

### Preparation of the KP films

The KGM/PDADMAC ratios were 100/0, 90/10, 80/20, 70/30, 60/40, 50/50, 40/60, 30/70, 0/100 (w/w), relative to dry KGM, with a total mass of 1.0 g. The proper PDADMAC and KGM were dissolved in 20 and 80 mL distilled water, respectively and stirred vigorously to form a uniform solution and then both solutions were mixed. The mixture was stirred vigorously at 25°C for 1 h and degassed. Finally, it was poured on to glass plates and water evaporated at room temperature for 2 days. The films of different ratios above were coded as KP0, KP1, KP2, KP3, KP4, KP5, KP6, KP7, and KP10, respectively. The blend films containing more than 70% PDADMAC formed two phases to the naked eyes obviously and had little mechanical strength, so they were discarded.

### Characterization of the KP films

The densities (ρ) of the KP films were determined with the equilibrium sedimentation method,[22] which required the use of two miscible liquids in which the

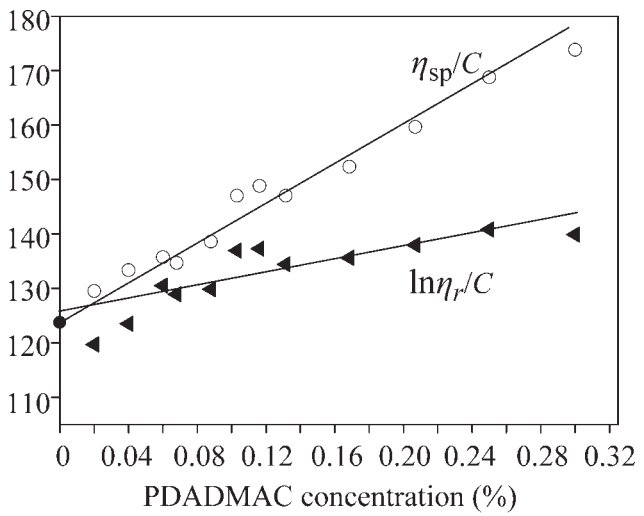


**Figure 2** Plots of $\eta_{sp}/C$ (○) and ln $\eta_r/C$ (◀) versus C of PDADMAC solutions, [η] (●) was the intercept of the curve of $\eta_{sp}/C$ versus *C* (T = 25 ± 0.1°C).

polymer sample did not dissolve or swell. It was also required that the sample float in one liquid and sink in the other. The KP film was placed in a glass vial with 3.0 mL of tetrachloride. Next, absolute ethanol was added dropwise until the sample began to sink. The dropwise addition of ethanol continued until the sample was suspended in solution, at which time the density of the solution was taken to be equal to the density of the KP sample. The density was determined by weighing 1.0 mL of solution. The average density was calculated from three separate density determinations.

Scanning electron microscopy (SEM) images of the films were taken with a microscope (JEOL 6700F, Japan). The films were cut into pieces and snapped, and then vacuum-dried. The surface and cross section of the films were sputtered with gold, and then observed and photographed.

X-ray diffraction (XRD) patterns were recorded on an X-ray diffraction instrument (XRD-6000 Shimadzu, Japan), by using CuKα radiation (λ = 0.1542 nm) at 40 kV and 30 mA with a scan rate of 4°/min. The diffraction angle ranged from 10° to 50°.

IR spectra of the films were recorded using a Fourier transform infrared (FTIR) spectrometer (Nicolet 170SX, USA) with attenuated total reflection instruments for investigation intermolecular interaction. The films were taken on the flat sheet and data were collected over 64 scans with a resolution of 4 $cm^{-1}$ at room temperature.

DSC was performed using a Netzsch DSC 200 PC at a heating rate of 10°C/min under nitrogen atmosphere. The temperature ranged from 20 to 500°C.

Thermal gravimetric measurements were performed using Netzsch STA 449C instrument (Germany) under a nitrogen atmosphere with a flow capacity of 30 mL/min. The scan was carried out at a heating rate of 10°C/min from 20 to 500°C. The sample weight was about 8-10mg and analyzed using α-$Al_2O_3$ crucible.

Tensile strength ($\sigma_b$) and elongation ($\epsilon_b$) at break of the films were measured on a versatile electron tensile tester (CMT-6503, Shenzhen SANS Test Machine, China) with a tensile rate of 5 mm/min. The size of the films strips was 70 × 10 × 50 $mm^3$ (length × width × distance between two clamps). The mean values of $\sigma_b$ and $\epsilon_b$ were obtained from five replications, respectively.

### Film-coating preservation experiment

The method was according to our previous work. The film of KP2, which has the best mechanical properties and miscibility, was chosen for testing. The proper PDADMAC and KGM with the composite ratio of 20:80 by solid weight were dissolved in distilled water respectively, and stirred vigorously to form a uniform solution, and then both solutions were mixed. The mixture was degassed after vigorous stirring for about 1 h. Fruits of lichi and grapes were classified into several groups. Every group contained 10 fruits. They were immersed in the blend solution for 2 min and then dried in air to allow a dry smooth film to form on the surface of fruit at room temperature (about 32°C) for 2 h. Both the experimental group and the control group were preserved in the open at room temperature at relative humidity of 65%. The preserve duration was 7 days. Every day, the change of the surface color of the fruit was observed. The weight loss rate of the lichi and grapes was calculated by

$$\text{Weight loss} = (W_0 - W)/W_0 \times 100\% \quad (1)$$

where $W_0$ and $W$ are the original weight and measured weight of the whole group after preservation, respectively. The rot rate of fruits was calculated by

$$\text{Rot rate of fruits} = N_r/N \times 100\% \quad (2)$$

where $N_r$ and $N$ are the number of rotten fruits after preservation for 7 days and that of total fruits, respectively.

## RESULTS AND DISCUSSION

### Miscibility between KGM and PDADMAC in the blend films

Usually, in a polymer blend, where there is no adhesion between the polymer interface and no molecular mixing at the phase boundary, the densities of the blend would be expected to follow the additivity rule of mixtures.[23] The densities measured from the volume density of the KP films as a function of PDADMAC content are shown in Figure 3. It can be

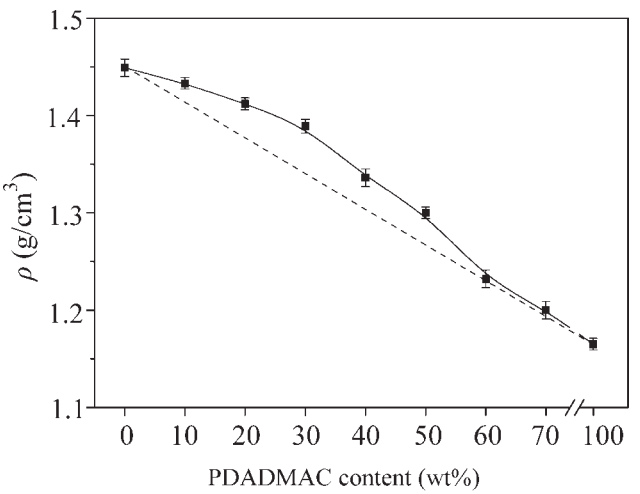


**Figure 3** Dependence of the density on PDADMAC content for the KP films [the dashed line (-----) was expressed to the theoretical density of the KP films].

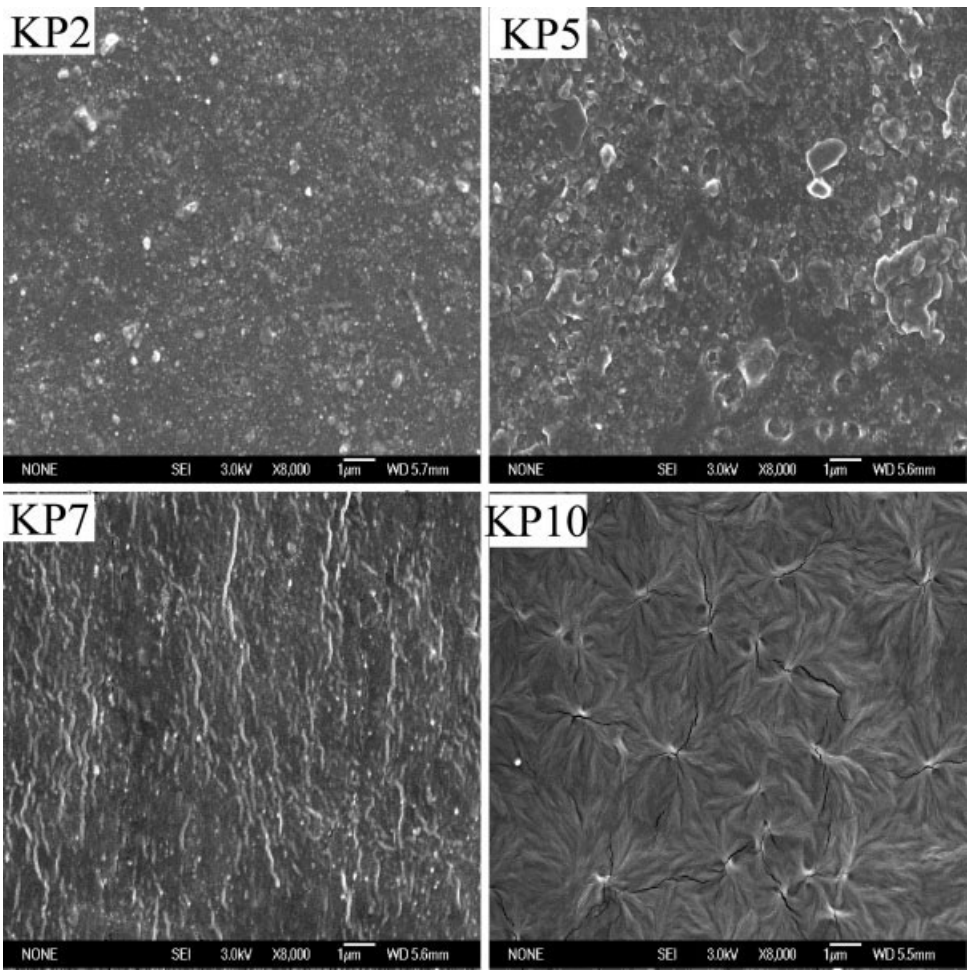


**Figure 4** SEM images of the surfaces of the KP films.

seen that when the PDADMAC content was less than 70 wt %, the experiment density values of the KP films were obviously higher than that theoretically calculated. These indicated a strong adhesion existence between KGM and PDADMAC molecules. The result can be explained that PDADMAC molecules penetrated into KGM matrix to bind together, led to a reduction of the free volume of the blend films. Therefore, the KP films possessed higher densities than that of pure KGM and PDADMAC. It can be predicted that PDADMAC and KGM have good miscibility in the blends when the PDADMAC content was less than 70 wt %. The SEM images of the blends would confirm the result directly.

### Morphology of the films

Figure 4 shows the SEM images of the surfaces for the blend films KP2, KP5, KP7, and KP10. The image of KP10, the pure functional polymer PDADMAC, showed a typically crystal morphology. From the image of KP7, it was found that the shape of the surface morphology changed from the radiation to the ordered line, but still homogeneous and smooth. As to the image of KP5, most of the morphology was homogeneous and there were some assembled particles in the homogeneous matrix. As to KP2, a homogeneous morphology was displayed and the assemble particles became small and uniform. It can be seen that as the KGM content increased, the morphology of the blend film surfaces changed from being smooth to becoming microphase separated, implying that the two kinds of polymers had a good miscibility, which may have led to the decrease of crystal.[24]

It was very interesting that all of the blends had the homogeneous morphology, but different microstructures were displayed. Both the natural and synthetic polymers were prone to water-soluble, so it was not strange that the homogeneous morphology was observed. Therefore, there must exist interactions between the two polymers that resulted in the different miscibility and microstructure of the blends. The highest miscibility occurred when the PDADMAC content was 20 wt %. With the increasing of KGM content, the intermolecular interaction

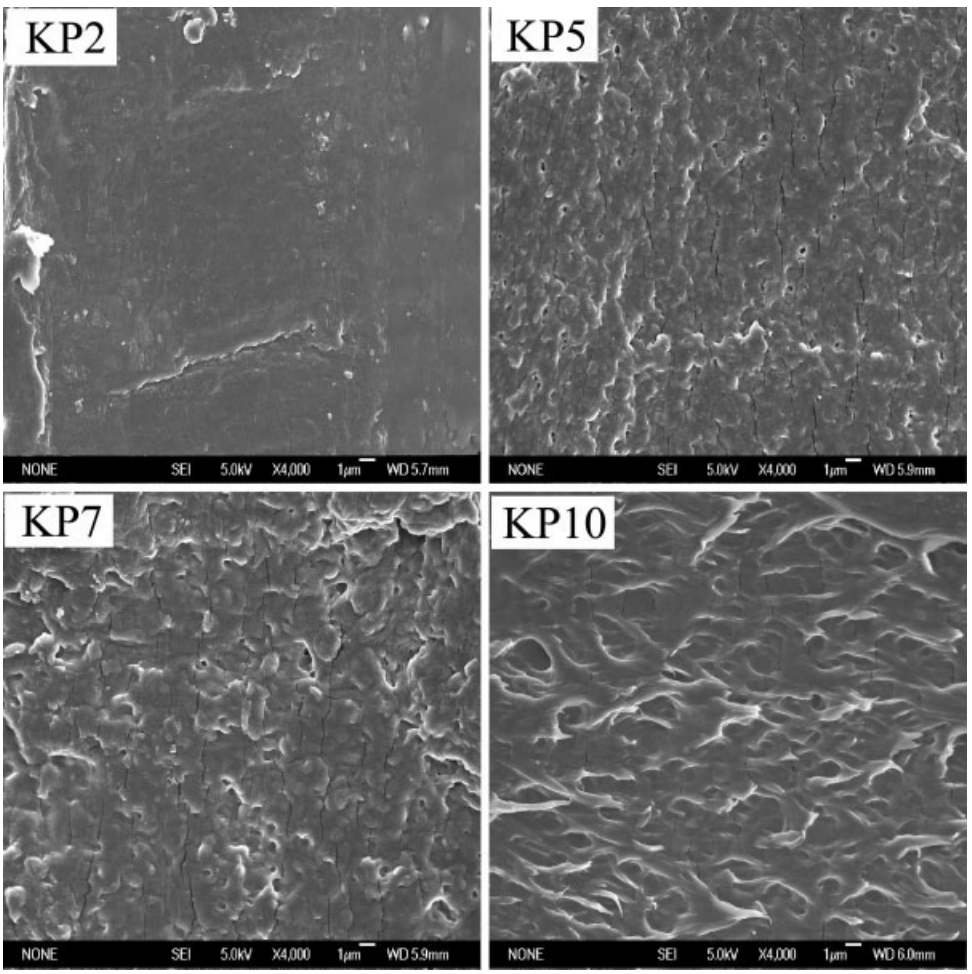


**Figure 5** SEM images of the cross sections of the KP films.

restrained the crystal behavior of PDADMAC, so the different microstructures occurred. The interaction between the two polymers will be discussed later.

Figure 5 shows the SEM images of the cross sections of the films. All the films displayed uniform and dense morphology, but the morphology changed from smooth to rough with the increase of the PDADMAC content. Therefore, we predicted that PDADMAC and KGM had good miscibility in the blend films, but the PDADMAC content affected the microstructure of the blends.

XRD was used to probe the crystal behavior of the blends. X-ray diffraction patterns of the KP blend films are shown in Figure 6. The pattern of KGM showed a broad peak at $2\theta = 21.3^\circ$, and several small and weak peaks appeared at $14.40^\circ$, $37.85^\circ$, and $44.08^\circ$. The pattern of PDADMAC showed a broad peak and a stronger peak at $2\theta = 16.39^\circ$, $22.04^\circ$, $27.57^\circ$, and $31.92^\circ$, respectively. If KGM and the other polymer had low compatibility, each polymer would have its own crystal region in the blend films, so X-ray diffraction patterns would be expressed simply as mixed patterns of KGM and the

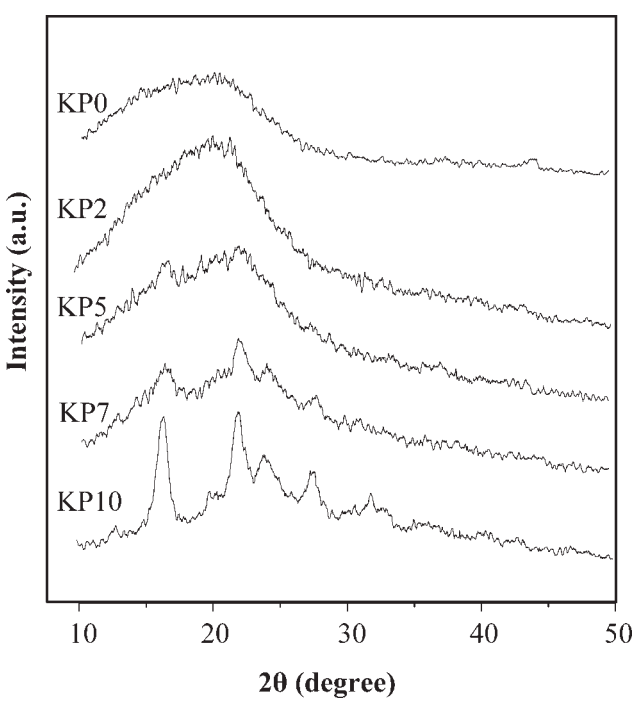


**Figure 6** X-ray diffraction patterns of the KP films.

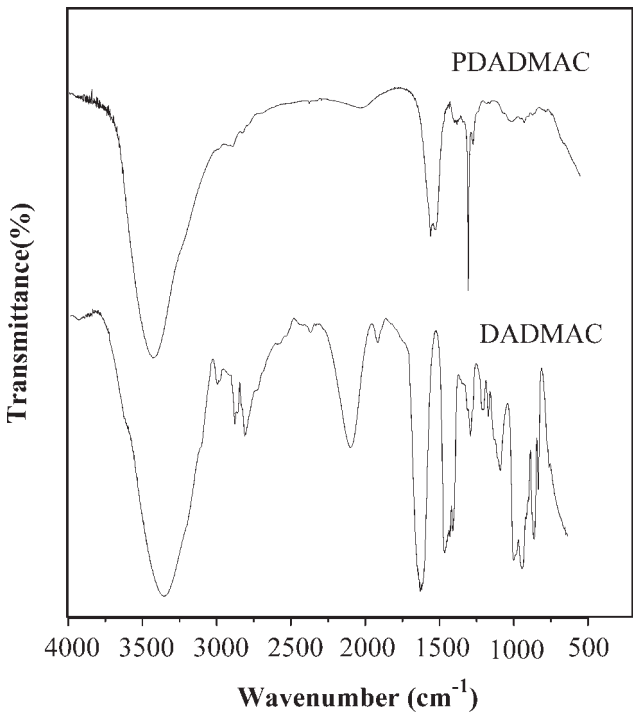


**Figure 7** IR spectra of DADMAC and PDADMAC.

other polymer with the same ratio as those for blending.[19] Fortunately, the case did not occur in the blend films. Comparing the patterns of KP2, KP5, and KP7 to that of KP10, it was obvious that the diffraction peak at 16.39°, 22.04°, 27.57°, and 31.92° became weaker with the reduction of PDADMAC down to 20% and hardly appeared finally. It can be explained that the intermolecular interactions between KGM and PDADMAC made the PDADMAC molecules dispersing into the KGM matrix and the crystal behavior of PDADMAC was restrained. Consequently, the crystal of PDADMAC decreased and good blend miscibility occurred. This result supported the SEM conclusion that good miscibility existed between KGM and PDADMAC when the PDADMAC content was less than 70% and the highest miscibility appeared when the PDADMAC content was 20%.

### Infrared

IR spectra were used to characterize the structure of the substances and investigate the interaction between the two polymers. The IR spectra of the DADMAC monomer and polymer are shown in Figure 7. As to the monomer, a strong peak at 3440 and 1649 $cm^{-1}$ corresponded to the stretching and distortion of hydroxyl, owing to the hygroscopic nature of the monomer. The peak at 2945, 2830, 1478, and 1385 $cm^{-1}$ assigned to methyl and methylene groups. The band at 3012, 1638, and 958 $cm^{-1}$ belonged to the ethylene stretching and distortion. The band at 1640 $cm^{-1}$ related to the vibration of $NR_4$[25] overlapped with that of the ethylene stretching. From the IR spectra of PDADMAC, it can be seen that the characteristic absorption bands around 1640 and 958 $cm^{-1}$ became weak. The reason was that the ring forming should reduce the bond energy.[26] It indicated that the polymerization performed. The results were in agreement with the report.[27]

Figure 8 shows the IR spectra of the OH stretching region of the KGM and blend membranes. It can be seen that the absorption band around 3330 $cm^{-1}$ corresponding to the stretching of hydroxyl for KP0 narrowed and gradually shifted to a high wave number 3407 $cm^{-1}$ and became strong when KGM blended with PDADMAC. It indicated that an intramolecular hydrogen-bonded state of pure KGM was interrupted in the blend films. Figure 9 shows the IR spectra of the KGM and blend membranes in the wavelength region 1800–800 $cm^{-1}$. Under electrostatic interaction, the bond of C—O—C at 1020 $cm^{-1}$ for KP0 shifted to higher wavenumbers in the blend films of KP2, KP5, and KP7. The distortion vibration of methyl at 1478 $cm^{-1}$ for PDADMAC was weakened and gradually shifted to lower wavenumbers with the increase in content of KGM in the blend films. At the same time, the characteristic absorption bands at 1640 and 958 $cm^{-1}$ in the blend films became weak too. These effects were a consequence of the electronic distribution changes in the molecular structure of PDADMAC and KGM, resulting

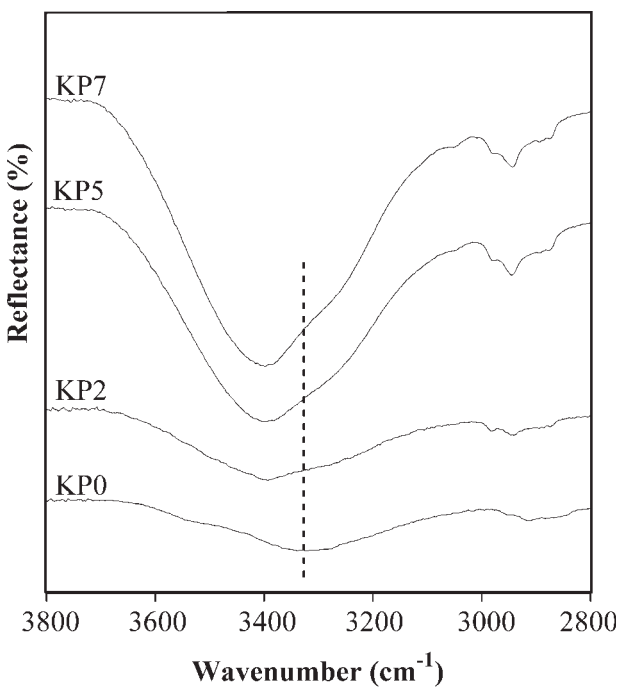


**Figure 8** IR spectra of the KP films in the wavelength region 3800–2800 $cm^{-1}$.

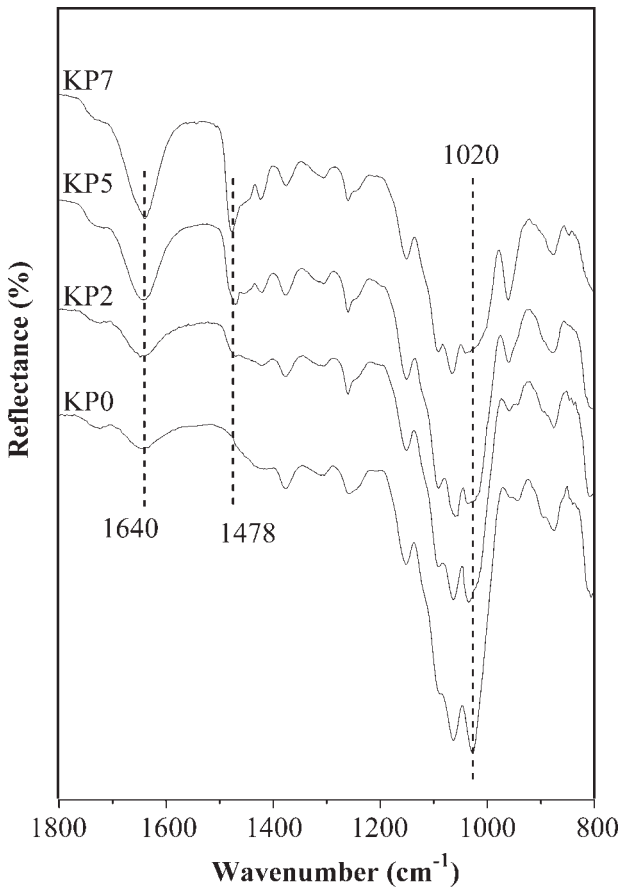


**Figure 9** IR spectra of the KP films in the wavelength region 1800–800 $cm^{-1}$.

from the strong electrostatic interaction. Furthermore, the characteristic absorption bands of mannose in the blend films at 874 and 805 $cm^{-1}$ became weaker with the increase in content of PDADMAC in the blend films, indicating that strong electrostatic interaction exists between KGM and PDADMAC.

## Thermal stability

Figure 10 shows the TG thermograms of the films, and the detailed thermogravimetric data of the films are displayed in Table I. All the films had weight loss of about 13% in the range of 50–120°C, owning to the release of water molecules from the films. With the increase of the temperature, the film of pure KGM and PDADMAC began the step of maximum weight loss at 208.1 and 335.0°C, while the films of KP2, KP5, and KP7 showed at 252.3, 235.4, and 223.5°C, respectively. It was found that the onset temperatures of weight loss for the blend films were higher than that of pure KGM and lower than pure PDADMAC. The case resulted from the blending with synthetic functional polymers could improve the thermostability of the natural polymer. It was also found that the onset temperatures of weight

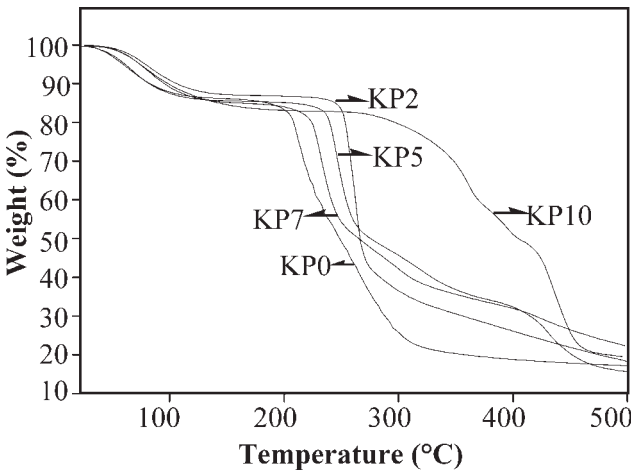


**Figure 10** TG thermograms of the KP films.

loss for the blend films increased with the decrease of the PDADMAC content, the order of thermostability of the films was KP2, KP5, and KP7. The film of KP2 showed two steps of weight loss similar to that of KP0, while the films of KP5 and KP7 showed three steps similar to that of KP10. The greatest weight loss of the films was attributed to the decomposition of PDADMAC and KGM.

The DSC curves of the films are displayed in Figure 11. The curves of all the films showed an endothermic peak at 80–104°C, which was attributed to the loss of moisture. The exothermic peak around 228°C for the film KP0 resulted from the thermal degradation of KGM. The exothermic peak around 305°C for the film KP10 was attributed to the thermal degradation of PDADMAC. The DSC curves of the films of KP2, KP5, and KP7 showed exothermic peak at 264.4, 253.7, and 258.6°C. It can be seen that the film KP2 has the highest thermostability of the blend films, which was caused by the good miscibility. It was found that the DSC curves of KP5, KP7,

**TABLE I**
**Thermogravimetric Data of the KP Films**

| Sample | Decomposition stage | Temperature range (°C) | Weight loss (%) |
|---|---|---|---|
| KP0 | 1 | 40.5–97.3 | 13.02 |
| | 2 | 208.1–310.0 | 65.34 |
| KP2 | 1 | 60.0–110.8 | 12.43 |
| | 2 | 252.3–270.4 | 55.23 |
| KP5 | 1 | 48.2–102.0 | 13.40 |
| | 2 | 235.4–353.4 | 40.17 |
| | 3 | 412.4–449.6 | 12.72 |
| KP7 | 1 | 59.5–113.5 | 13.95 |
| | 2 | 223.5–333.7 | 47.32 |
| | 3 | 355.1–413.5 | 4.19 |
| KP10 | 1 | 57.0–121.5 | 14.05 |
| | 2 | 335.0–369.5 | 21.21 |
| | 3 | 389.4–403.8 | 5.19 |
| | 4 | 425.2–458.9 | 27.36 |

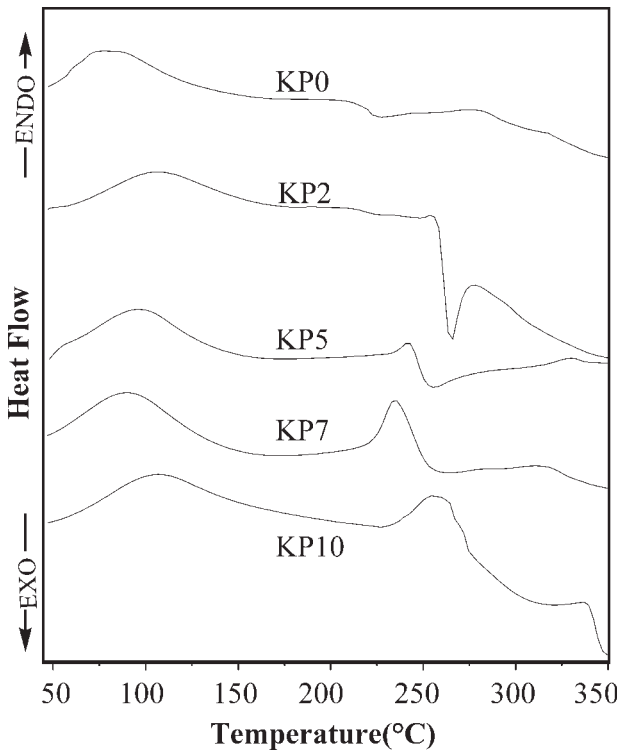


**Figure 11** DSC thermograms of the KP films.

and KP10 displayed obvious endothermic peaks around 232.3–254.9°C, and the curve of the film KP2 showed a weak endothermic peak around 251.7°C, which were attributable to the melting of the crystal phase in the blend films. These results of the TG and DSC analysis are in agreement with results of SEM and X-ray analysis.

## Mechanical properties

Because polymer materials, such as films, may be subjected to various kinds of stress during use, the determination of the mechanical properties involves not only scientific but also technological and practical aspects.[28] The blank bars in Figure 12 show the effect of the PDADMAC content on the stress-at-break ($\sigma_b$) of the KP blend films. It can be seen that the addition of PDADMAC to KGM was effective on enhancing the mechanical properties of the blend films. The strain-at-break of the pure KGM was 67.07 MPa. With the increasing of the PDADMAC content, the tensile strength of the blends increased and the maximum value of 106.5 MPa was achieved at the PDADMAC content of 20 wt %, and then decreased. The result was higher than that of ever reports and the remarkable increase in the tensile strength of the KP blend films indicated the presence of the intermolecular interactions between KGM and PDADMAC. With the increase of the PDADMAC content, since the intermolecular interactions were not strong enough to destroy the crystal behavior of PDADMAC, the tensile strength of the blend films decreased. The case agreed with the results of SEM and XRD analysis.

The curve with black dots in Figure 12 shows the dependence of the strain-at-break ($\epsilon_b$) on the PDADMAC content for the KP films. The strain-at-break of the pure KGM was 6.17%. When the PDADMAC content was less than 20 wt %, the alteration of the breaking elongation expressed a tendency similar to that of the tensile strength for the blend films, and also reached the maximum 32.04% at 20 wt % PDADMAC content, then decreased. But when the PDADMAC content was higher than 30 wt %, the breaking elongation began to increase mildly with the increasing of the PDADMAC content. The reason was that the crystal phase of PDADMAC would be oriented under the stress. After all, the blend film KP2 had better integrate mechanical properties than others.

## Film coating preservation

Lichi is an abundant fruit in the south of China, while grapes are another abundant fruit in the northwest of China. Both of them rot easily during preservation and transport, and there is magnitude expense. Therefore, it is necessary to find a preservative to delay the rot. The permeability of water, oxygen for the preservative is important. Therefore, the water loss rate and the rot rate of the fruits are used to estimate the performance of the material. The fruits were purchased from the market. The blend film KP2, which had the best properties of the blends, was chosen as the preservative. Table II shows the changes that the fruits undergo during preservation. The red color of Lichi for control groups was completely lost within a day and fruits

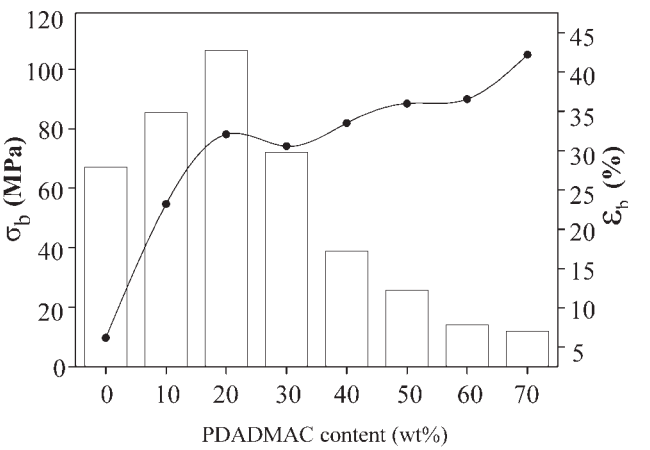


**Figure 12** Dependence of the $\sigma_b$ (bars) and $\varepsilon_b$ (●) on PDADMAC content.

**TABLE II**
**Physical Changes of Lichi and Grapes with Various Preservation Times**

| | Lichi | | Grapes | |
|---|---|---|---|---|
| Time (day) | Experimental group (blend films) | Control group | Experimental group (blend films) | Control group |
| 1 | No change (pericarp was red) | Color of pericarp became light brown | No change (pericarp was red) | Color of pericarp became dark |
| 2 | Red color faded away | Color of pericarp became brown | No change (pericarp was red) | Fruits softened |
| 3 | Fresh red color of pericarp lost | Fruit was rigid and pinched when pericarp appeared crack | Pericarp was deep red | Fruits shrinked |
| 4 | Color of pericarp became brown completely | Fruit emitted a strong sour smell | Fruits softened | Fruits shrinked sharply, dent appeared on pericarp |
| 5 | Percicarp cracked, and fruits became rigid | Fruit was mildewed and flowed liquid with bad smell | Fruits shrinked | Pericarp cracked, shrinked sharply |
| 6 | Crack of pericarp increased | | Dent of Pericarp appeared | Fruits softened and shrinked sharply |
| 7 | Fruit emitted liquid with bad smell | | Fruits shrinked | Liquid flowed out |
| Rot rate | 10% | 90% | 0% | 50% |

became mildewed and rotted away completely by the fourth day, while that of the experimental groups showed slowed tendency. The rot rate of Lichi for experimental groups and control groups were 10 and 90%, respectively. As to grapes, it was interesting that there was no rot for the experimental groups and the rot rate for the control groups was 50%. We tasted the grapes in the experimental groups and they were sweet.

Figure 13 shows the weight loss rate dependence on preservation time. It is obvious that the weight loss rate of the fruit with coating was lower than that of the fruit without coating. This result indicated that the blend film had good water-holding ability. After all, the blend films had good preservation ability and were safe to human's health.

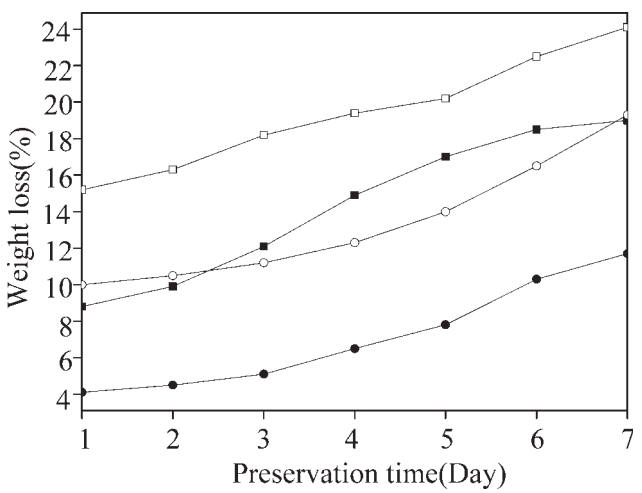


**Figure 13** Dependence of weight loss rate of the fruits on preservation time (□ no coated lichi; ■ coated lichi; ○ no coated grapes; ● coated grapes).

## CONCLUSIONS

A novel preservative film was prepared by blending KGM and PDADMAC in aqueous system. The results of the density determination, SEM, and XRD predicted that there was good miscibility between KGM and PDADMAC in the blends when the PDADMAC content was less than 70 wt % and the highest miscibility appeared when the PDADMAC content was 20%. ATR-IR showed that strong intermolecular hydrogen bond interaction occurred between the negative charge groups of KGM and the quaternary ammonium groups of PDADMAC in the blends. The tensile strength and the break elongation of the blends were improved largely to 106.5 MPa and 32.04% when the PDADMAC content was 20 wt %. The thermal stability of the blends was higher than the natural polymer. The film-coating preservation experiments with lichi and grapes showed that the blend film KP2 had excellent water-holding and preservative ability. From the work, we predict that the blend film KP2 has super integrated properties as preservative materials and has potential applications in biomedical fields. We should make further researches in the future.

## References

1. Maeda, M.; Shimahara, H.; Sugiyama, N. Agric Biol Chem 1980, 44, 245.
2. Chun, S. Y.; Kim, H. I.; Yoo, B. Food Sci Biotechnol 2006, 15, 589.

3. Li, B.; Peng, J. L.; Yie, X.; Xie, B. J. J Food Sci 2006, 71, C174.
4. Cheng, L. H.; Abd Karim, A.; Norziah, M. H.; Seow, C. C. Food Res Int 2002, 35, 829.
5. Cuna, M.; Alonso-Sande, M.; Remunan-Lopez, G.; Pivel, J. P.; Alonso-Lebrero, J. L.; Alonso, M. J. J Nanosci Nanotechnol 2006, 6(9/10), 2887.
6. Alvarez-Mancenido, F.; Braeckmans, K.; De Smedt, S. C.; Demeester, J.; Landin, M.; Martinez-Pacheco, R. Int J Pharma 2006, 316, 37.
7. Alonso-Sande, M.; Cuna, M.; Remunan-Lopez, C. Macromolecules 2006, 39, 4152.
8. Yu, H. Q.; Huang, A.; Xiao, C. B. J Appl Polym Sci 2006, 100, 1561.
9. Chen, L. G.; Liu, Z. L.; Zhuo, R. X. Polymer 2005, 46, 6274.
10. Cheng, L. H.; Abd Karim, A.; Seow, C. C. J Food Sci 2006, 71, E62.
11. Tian, D. T.; Hu, W. B.; Zheng, Z.; Liu, H. B.; Xie, H. Q. J Appl Polym Sci 2006, 100, 1323.
12. Li, B.; Xie, B. J. J Appl Polym Sci 2004, 93, 2775.
13. Torres, J. A.; Motoki, M.; Karel, M. J Food Process Preserv 1985, 9, 75.
14. Li, B.; Kennedy, J. F.; Peng, J. L.; Yie, X. B.; Xie, J. Carbohydr Polym 2006, 65, 488.
15. Lu, J.; Xiao, C. B. J Appl Polym Sci 2007, 103, 2954.
16. Xiao, C. B.; Gao, S. J.; Wang, H.; Zhang, L. N. J Appl Polym Sci 2000, 76, 509.
17. Xiao, C. B.; Gao, S. J.; Zhang, L. N. J Appl Polym Sci 2000, 77, 617.
18. Xiao, C. B.; Lu, Y. S.; Liu, H. J.; Zhang, L. N. J Appl Polym Sci 2001, 80, 26.
19. Xiao, C. B.; Lu, Y. S.; Gao, S. J.; Zhang, L. N. J Appl Polym Sci 2001, 79, 1596.
20. Liu, C. H.; Xiao, C. B. J Appl Polym Sci 2004, 93, 1868.
21. Wandrey, C.; Hernandez-Barajas, J.; Hunkeler, D. Adv Polym Sci 1999, 145, 123.
22. Kirker, K. R.; Prestwich, G. D. J Polym Sci Part B: Polym Phys 2004, 42, 4344.
23. Kim, S. C.; Klempner, D.; Frisch, H. L. Macromolecules 1976, 9, 258.
24. Yang, G.; Zhang, L.; Feng, H. J Membr Sci 1999, 161, 31.
25. Lin, X. J.; Zhong, A. Y.; Chen, D. B.; Zhou, Z. H.; He, B. B. J Appl Polym Sci 2003, 87, 369.
26. He, L.; Hu, J. M.; Ye, Y.; Shi, H.; Niu, F.; Gu, Y. H.; Niu, C. R. Chem J of Chin Univ 1999, 20, 1362.
27. Xujie, Y.; Xin, W.; Hengzhi, W. J Appl Polym Sci 2003, 87, 1957.
28. Freddi, G.; Romano, M.; Massafra, M. R.; Tsukada, M. J Appl Polym Sci 1995, 56, 1537.